Introduction

Many engineering problems require accurate estimates of stress and strain conditions. Shear wave velocities provide essential information about elastic moduli, which are indispensable material properties when numerically describing and modelling a volume of earth. Shear-wave velocities can be estimated using several different seismic surface-wave methods. One of these methods is the passive version of the multichannel analysis of surface-wave (MASW) technique (Park et al. 2004). Passive surface waves generated from ambient noise (mainly vehicle traffic) are generally low frequency and can have wavelengths that reach tens to hundreds of meters (Okada, 2003). The passive surface wave method therefore has the potential to reach investigation depths significantly greater than active sources and can be effectively used in very noisy settings.

In this study orientated arrays (Leitner et al., 2011) are investigated in a noisy area (Figure 1a), to test the sensitivity of their dispersion curves, when high and low amplitude signals are coming from different directions.

Data acquisition

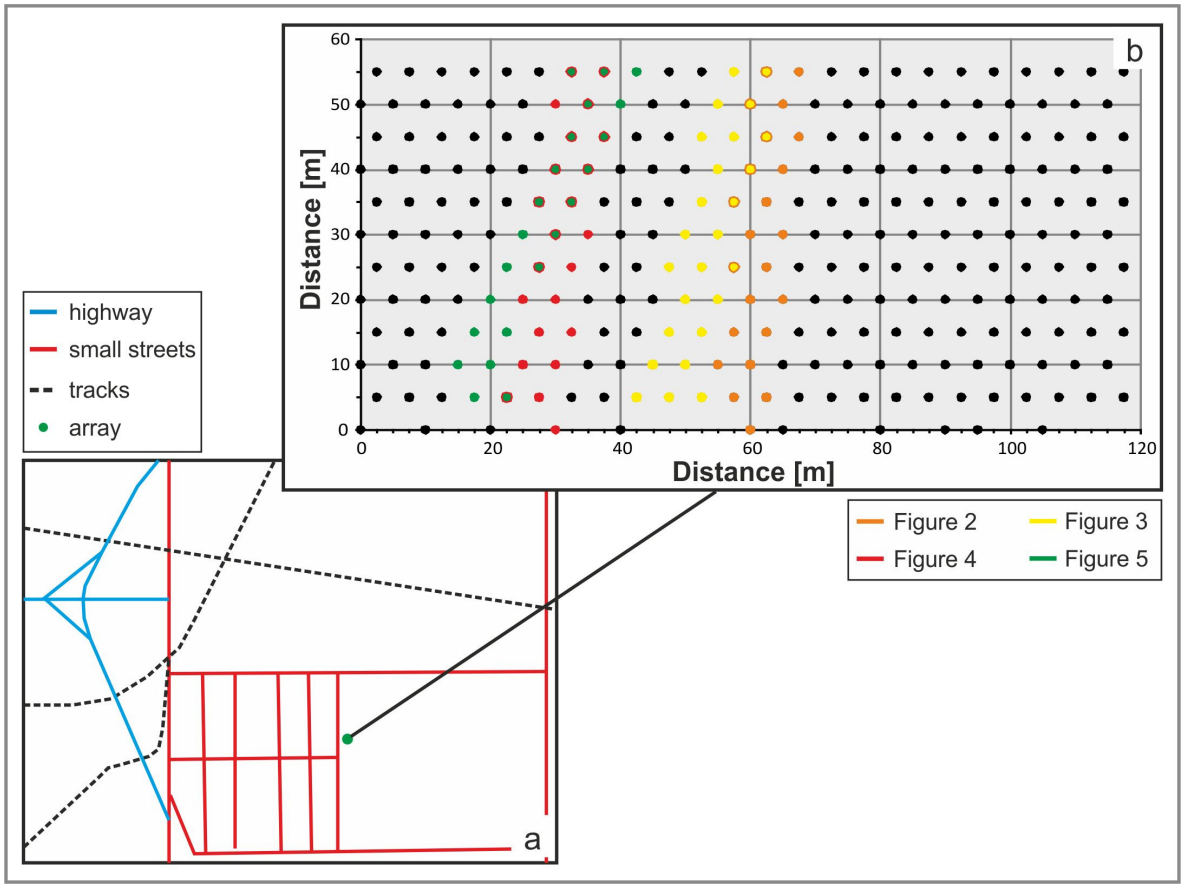

Figure 1 *a) Surroundings of the spread, b) receiver layout with sub array of figure 2 to figure 5.*

An array of 275 receivers was deployed in a 2-D spread (Figure 1b). The 4.5 Hz vertical geophones were planted at 12 WE-lines with each 24 receivers. The receiver spacing in a WE-line was 5 meters, the lines were 5 meters apart, but every second line was shifted 2.5 meters east. Railroad tracks, highways and streets (Figure 1a) around the array provided a wide range of azimuthal orientations. Each record was 32 sec long with a sample interval of 2 msec.

Data processing

Data have been processed using the dispersion imaging scheme described by Park et al. (2004).

As extension to the former procedure, for this work, the data were scanned in time windows for the angle of maximum incoming energy at each frequency of interest. Time window quality increases with the number of frequency intervals with the same angle of maximum incoming energy. Sub arrays, in dimensions of a rectangle, orientated in the angle of maximum energy, were scanned again for each frequency in a phase velocity azimuth diagram to check for any sub array maximum energy in the area of orientation angle. The energy is then stacked over the orientation azimuth with boundaries of 2 degrees.

For this study, data with energy mainly from one direction are compared with data that has confirmed maximum energy from a similar direction, but additional noise energy coming from other angles.

Results

Figures 2 to 5 show dispersion curves (part *a)* in each Figure) processed after the scheme discussed before from four different two second time windows. For each dispersion curve the distribution of energy for the processed time window is shown in an Azimuth – Frequency image (part *b)* in each Figure). The black dashed lines mark the angle of maximum incoming energy, based on which the sub spreads were orientated (Figure 1b) and energy was stacked (+-2 °). The red dashed lines assign the frequencies and energy distribution investigated in this study.

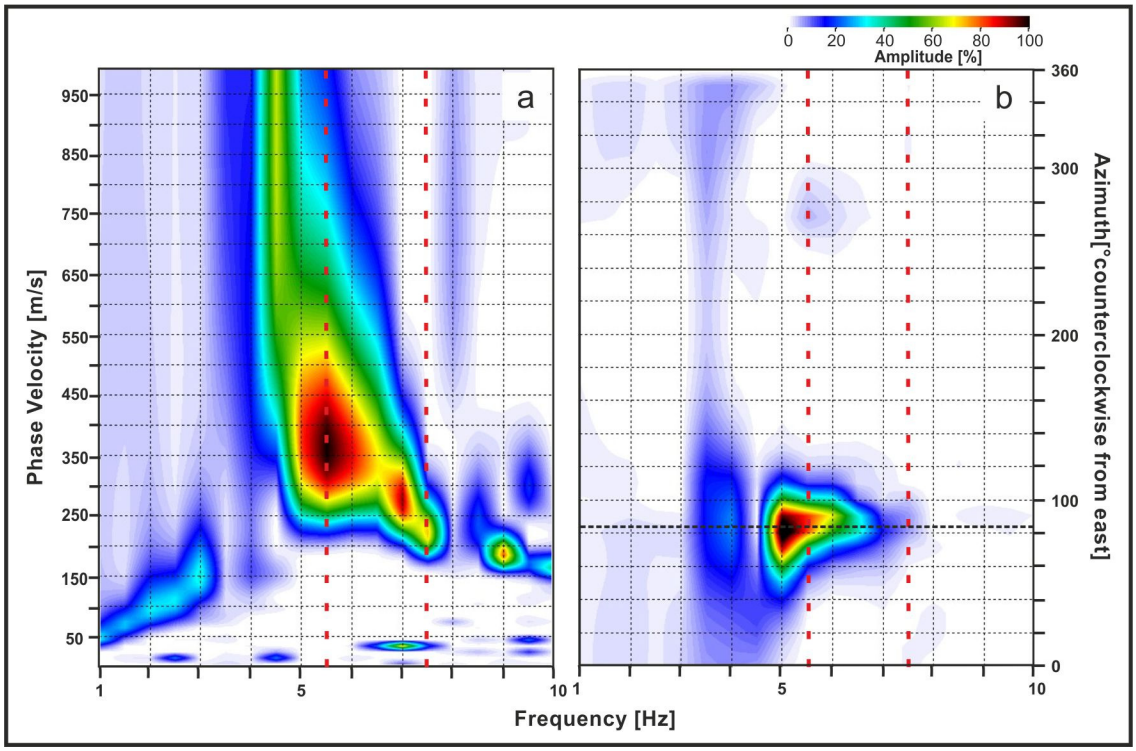

Figure 2 *a) Phase- velocity frequency image, b) Azimuth versus frequency diagram, black dashed line assigns angle of sub spread orientation (84°), red dashed lines mark the investigated frequencies and energy distributions.*

Figure 2b shows an energy concentration at an angle of about 84 ° counter clockwise from east, for the frequencies of interest (5 to 10 Hz, for lower frequencies the spread in N-S direction is to short).

For Figure 3b the energy distribution is more expanded, even if the maximum energy is similar to the former coming from 76°. Especially for the marked frequencies of 5.5 Hz and 7.5 Hz, a major part of energy is also coming from 10 to 100 °, and additionally a small percentage from 300 to 350°.

In the phase-velocity frequency diagram (Figure 3a) a maximum amplitude is evident at the frequencies of 5.5 and 7.5 Hz. This amplitude high is elongated and shifted to higher phase velocities, in comparison to the image in Figure 2. In Figure 2a the phase velocity amounts for 5.5 Hz to about

360 m/s and for 7.5 Hz the velocity is at 220 m/s. In Figure 3a both the 5.5 Hz and 7.5 Hz frequency intervals have a stretched amplitude distribution with a centre at about 450 m/s.

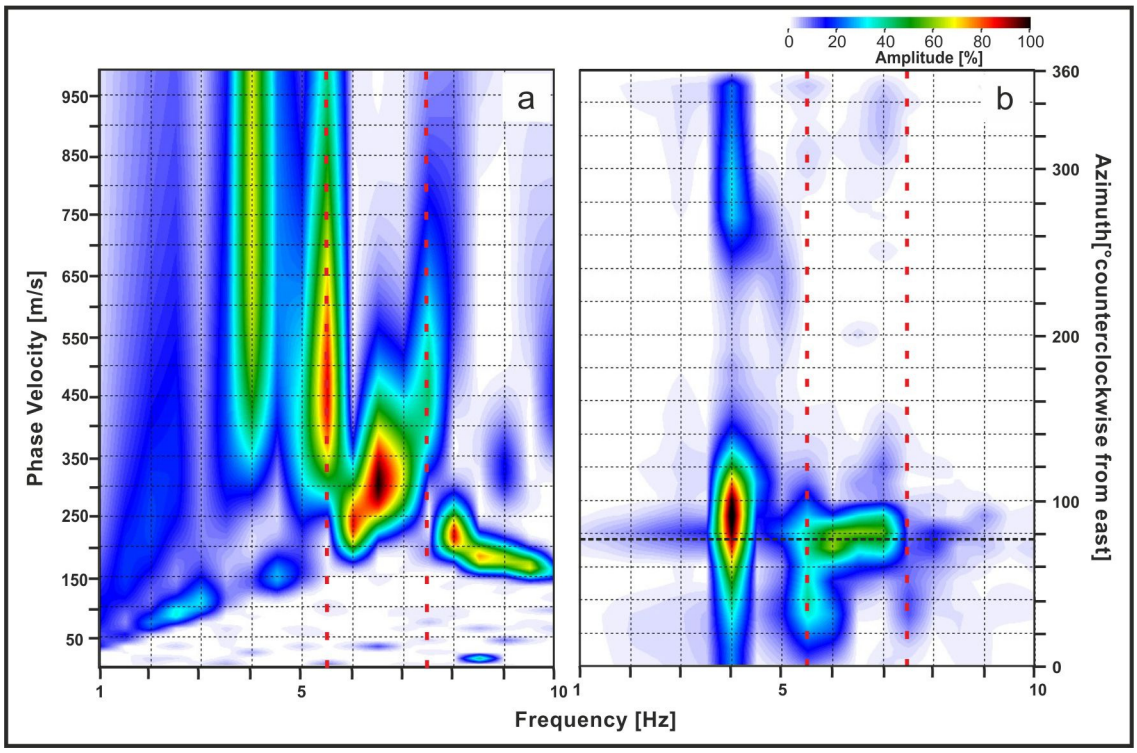

Figure 3 *a) Phase- velocity frequency image, b) Azimuth versus frequency diagram, black dashed line assigns angle of sub spread orientation (76°), red dashed lines mark the investigated frequencies and energy distributions.*

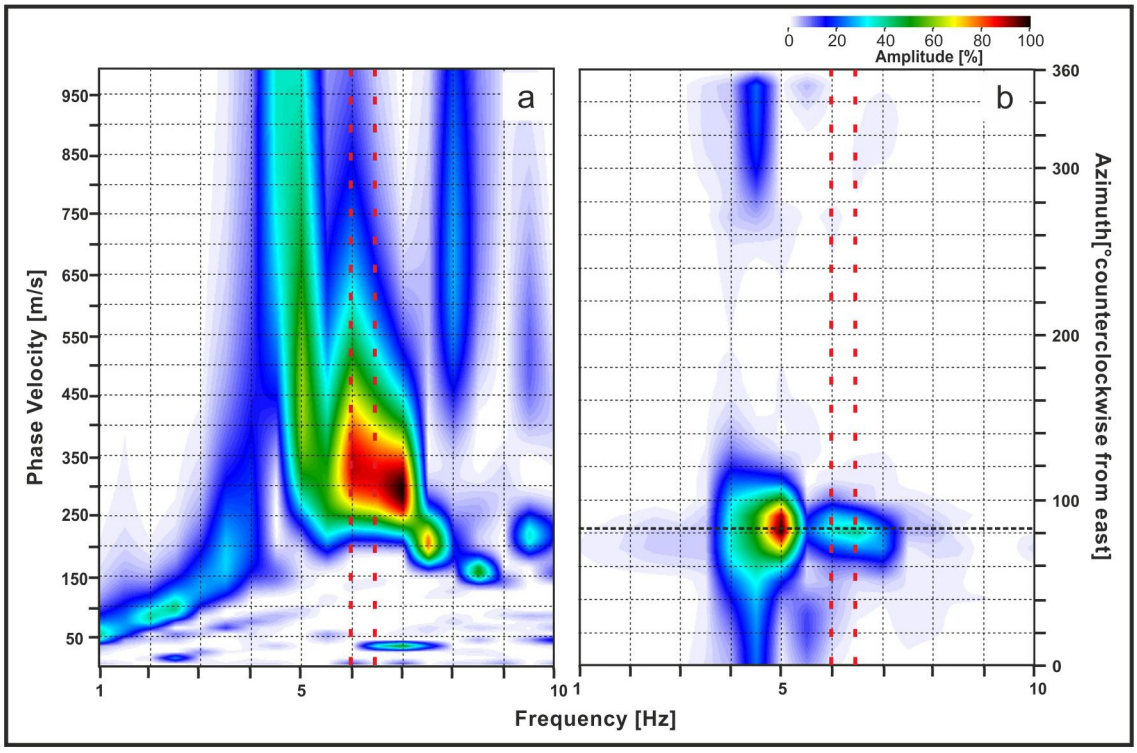

Figure 4 *a) Phase- velocity frequency image, b) Azimuth versus frequency diagram, black dashed line assigns angle of sub spread orientation (82°), red dashed lines mark the investigated frequencies and energy distributions.*

Figure 4b shows an energy concentration at an angle of about 82 ° counter clockwise from east for the frequencies of interest.

In Figure 5b the energy distribution is more expanded, even if the maximum energy is concentrated around 68°. Especially for the marked frequencies of 6 Hz and 6.5 Hz, the energy is more diffuse than in Figure 4.

In comparison to Figure 4a, the maximum amplitudes of the marked frequencies (6Hz and 6.5 Hz) of Figure 5a are stretched and have higher phase velocities. In Figure 4a the phase velocity for 6 Hz is about 325 m/s and for 6.5 Hz the velocity is at 310 m/s. In Figure 5a the 6 Hz frequency reaches a phase velocity of 350 m/s and the 6.5 Hz frequency has a stretched amplitude distribution with a centre at about 425 m/s.

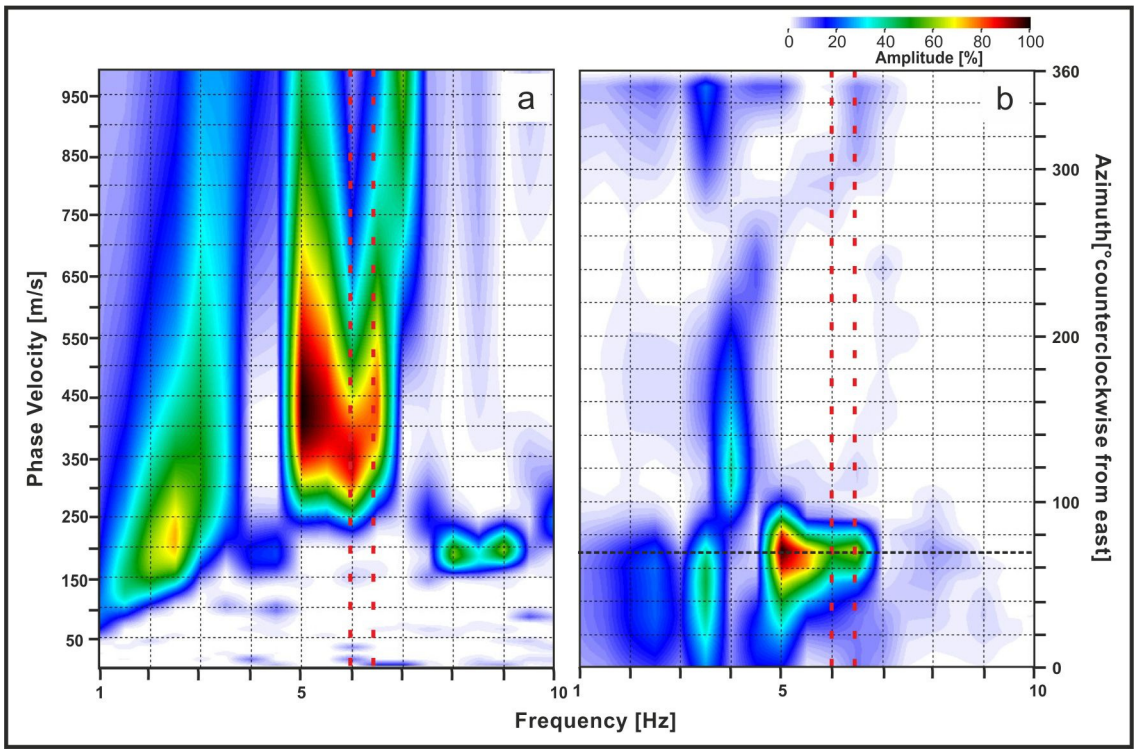

Figure 5 *a) Phase- velocity frequency image, b) Azimuth versus frequency diagram, black dashed line assigns angle of sub spread orientation (68°), red dashed lines mark the investigated frequencies and energy distributions.*

Conclusions

Even if a spread is orientated in the direction of maximum source energy and the energy is stacked over the optimal azimuth, background noise especially in the lower frequency ranges, induces a shift to a higher phase velocity on the phase -velocity frequency diagram and a deformation across the phase velocity. These can also be observed for the active method, when working with lower frequencies.

References

Okada, H. [2003] *The microtremor survey method*, Geophysical Monograph Series, **12**, SEG, Tulsa.

Park, C., R. Miller, D. Laflen, N. Cabrillo, J. Ivanov, B. Bennett, and Huggins, R. [2004] Imaging dispersion curves of passive surface waves. *SEG,* Extended Abstracts, 1357-1360.

Leitner, B., R. Miller and Ivanov, J. [2011] Optimal spread design for passive MASW. *Near Surface 2011.* Extended Abstract.